**SUPPORTING INFORMATION**

# Real-Time Label-Free Direct Electronic Monitoring of Topoisomerase Enzyme Binding Kinetics on Graphene

Laura Zuccaro[1,2], Cinzia Tesauro[2,3], Tetiana Kurkina[1], Paola Fiorani[2,4], Hak Ki Yu [5]

Birgitta R. Knudsen[3,6], Klaus Kern[1,7], Alessandro Desideri[2], Kannan Balasubramanian*[1]

[1] Max Planck Institute for Solid State Research, Heisenbergstr. 1, D-70569 Stuttgat, Germany.

[2] Department of Biology, University of Rome Tor Vergata, I-00133 Rome, Italy.

[3] Department of Molecular Biology & Genetics, Aarhus University, DK-8000 Aarhus, Denmark.

[4] Institute of Translational Pharmacology, National Research Council CNR, I-00133 Rome, Italy.

5 Max Planck Institute for Biophysical Chemistry, 37077 Goettingen, Germany.

[6] Interdisciplinary Nanoscience Center (iNANO), DK-8000 Aarhus, Denmark.

[7] Institut de Physique de la Matière Condensée, EPFL, CH-1015 Lausanne, Switzerland.

* *Corresponding author email:* b.kannan@fkf.mpg.de

---

## Terminology

In this study, we would like to detect the binding of the enzyme human DNA topoisomerase (hTop1) on to its substrate, which is double-stranded DNA containing the recognition sequence (GACTT*AG). This 'substrate' is not to be confused with 'substrate' used for denoting the silicon substrate. To avoid confusion we have used 'chip' for the latter.

In the area of biosensing, the terms 'analyte' and 'receptor' are often used. In our case the enzyme is the 'analyte' and the DNA is the 'receptor'. In order to avoid confusion with the terminology in biology (where 'receptor' could mean many other things), we have used the term 'capture DNA probe' to refer to the 'receptor' that is the double stranded DNA.

**DNA-functionalized graphene : Coupling DNA on to graphene.**

To detect the activity of hTop1, the graphene surface should be provided with selected DNA capture probes, which are the substrates specific for hTop1 catalysis. We perform the attachment of DNA in two steps as shown in the schematic in fig. S1(a) : first, the graphene surface is enriched with carboxyl groups through electrochemical modification, [1, 2] while in the second step amine-terminated DNA receptors are coupled to the carboxyl groups through carbodiimide coupling.[3] For the first step, *4*-aminobenzoic acid is electropolymerized on to the contacted graphene surface under oxidative conditions. Fig.S1(b) and S1(c) show AFM image of a graphene device before and after modification. Line profiles (as in fig. 2(d)) measured across the graphene edge show an increase in height of around 2 to 3 nm confirming the presence of polymeric deposit. This layer is non-covalently bound to the graphene surface as inferred from Raman spectra. [1, 3] In a second step, the exposed carboxylic groups are activated with ethylenediaminechloride/*N*-hydroxysuccinimide (EDC/NHS), which then react with the amino group at the 3'-end of the amino-DNA, forming amide linkages, resulting in a DNA-functionalized graphene surface. Residual activated COOH groups are blocked using 20mM ethanolamine. The presence of DNA can be confirmed by measuring the electrical characteristics. A representative example of the steady state field-effect response of the graphene device to the two steps of functionalization is shown Fig. S1(e). After the first step, the Dirac point shifts to more positive voltages signifying the introduction of acid groups, while after DNA attachment it shifts down indicating an increase in negative surface charge consistent with the presence of attached DNA receptors. [2] By deploying the same protocol on individual carbon nanotubes, we have shown that the DNA remains intact after the functionalization. [3] Sensor devices based on functionalized CNTs are not well-suited for the proposed study since the device-to-device variation in electrical characteristics is much higher compared to graphene devices. Moreover, due to the higher sensitivity to electric discharge, it is difficult to continuously monitor the sensor response of CNT devices over several hours.

**Figure S1**. **Attachment of capture DNA probes on to graphene**. (a) Reaction scheme showing the two steps for attaching amine-terminated DNA strands on to graphene. In a first step, 10mM *4*-aminobenzoic acid is electropolymerized on to the graphene surface in a solution of ethanol with 0.1 M lithium perchlorate. Subsequently, the carboxyl groups are activated using EDC/NHS, in order to covalently couple to the amine groups of the DNA receptor. (b,c) Atomic Force Microscopy (AFM) images of a typical graphene strip before (b)

and after (c) the electropolymerization. (d) Line profile across the graphene edge before (black curve) and after (red curve) the modification, showing an average increase in height of around 2.5 nm for this sample. (e) Field-effect characteristics of the graphene device before (black curve), after attachment of carboxyl groups (red curve) and after coupling of amino-functionalized DNA (blue curve), showing the device resistance $R_{gr}$ as a function of the applied electrochemical gate voltage ($V_{ecG}$).

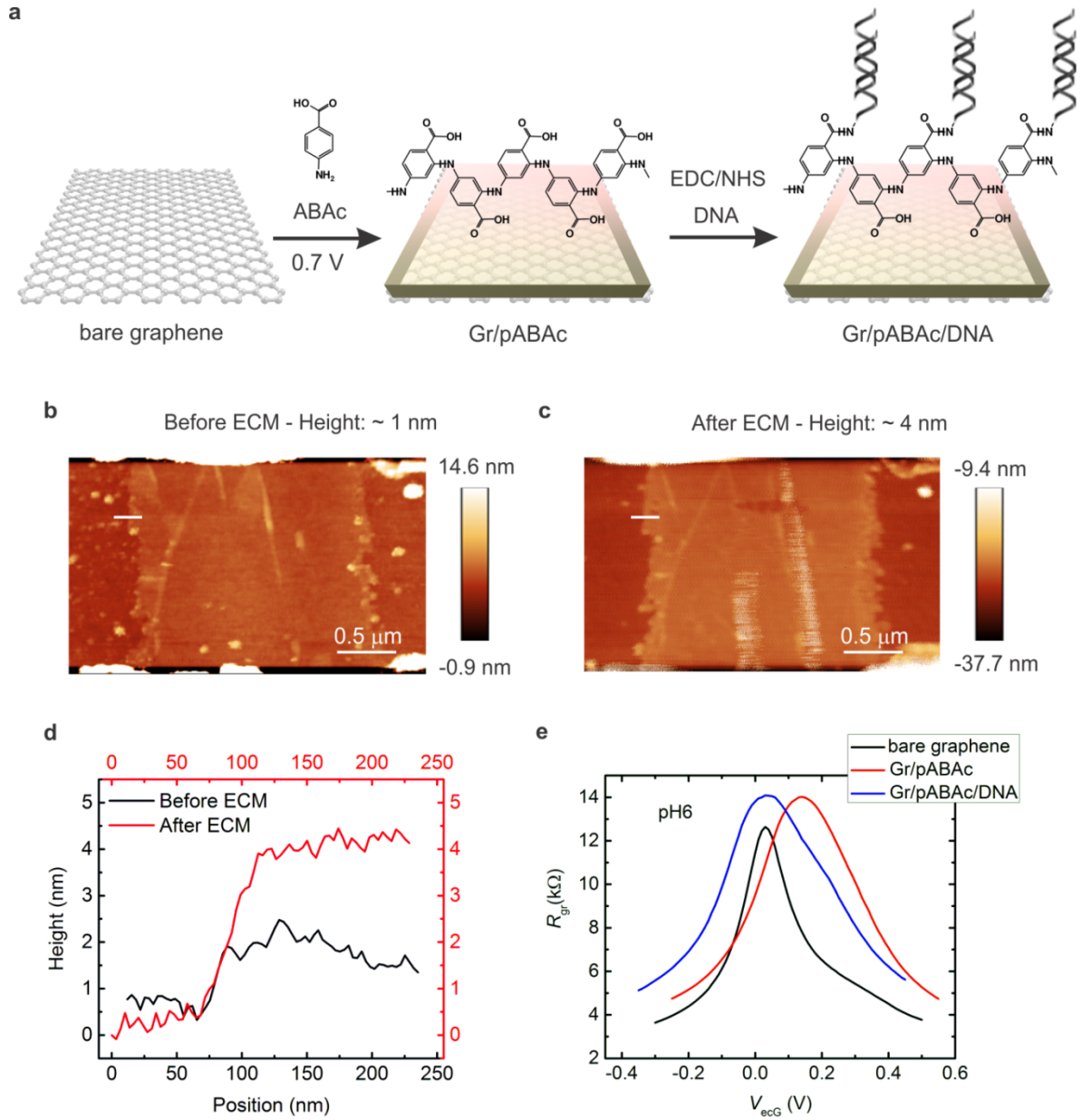

**Design of capture DNA probes**

The capture DNA probes (fig. 2(d-f)) used here have been designed in such a way that the cleavage and religation steps of topoisomerase activity can be decoupled in each other. For this purpose, it is necessary to control the progress of reaction after the cleavage step, which is achieved by using a phosphate group at the 5'-end and providing for a short nucleotide sequence downstream the cleavage site. The sequences *Topo Suicide* and *Topo Grissino* are very similar except that the latter is more stable than the former due to a higher melting point. Moreover, for *Topo Suicide* we need to perform the hybridization of the double strand either in solution or on the chip surface, whereas for the *Topo Grissino* this can be done simultaneously during the DNA coupling step. The *Topo Snack* has even a higher melting point, designed to ensure a tight coupling of the hTop1 on to it. Moreover the *Topo Snack* is composed of double-stranded DNA on both sides of the cleavage site, which is well documented to stimulate cleavage activity. [4]

**Comparison of active hTop1 and its heat-treated form (HIPO)**

hTop1 activity was assayed with a standard DNA relaxation assay. An equal amount of hTop1 or hTop1 HIPO (enzyme heat treated for 5 min. at 95°C) was incubated with 200 fmol of negatively supercoiled pUC18 plasmid DNA, in 20 µl of reaction buffer containing 20 mM Tris–HCl pH 7.5, 0.1 mM $Na_2EDTA$, 5mM mM $MgCl_2$, 5mM $CaCl_2$ and 150 mM KCl. The reaction mixture was incubated at 37 °C for 1 hour and terminated with 0.5% SDS (w/v). The samples were resolved in a 1% (w/v) agarose gel in running buffer containing 48 mM Tris, 45.5 mM boric acid, and 1 mM EDTA at 10 V/cm. After staining with ethidium bromide (0.5 µg/mL) and washing with water, the DNA bands were visualized using a UV transilluminator.

The ability of the enzyme to relax DNA is shown as the disappearance of the band of the supercoiled DNA (SC). Fig S2(a) clearly shows that the HIPO enzyme is completely inactive compared to the hTop1. The same proteins used in the relaxation activity assay (hTop1 and HIPO) were run on a 10 % SDS page and the bands were visualized by Comassie staining. As evident from fig S2(b), the heat treament doesn't change the mobility and integrity of hTop1 (compare hTop1 and HIPO) but only affects it's activity (fig S2(a)).

**Figure S2. DNA relaxation assay and protein gel**. Relaxation activity assay and SDS-PAGE of hTop1 and HIPO. (a) Relaxation activity of hTop1 and HIPO were assayed by

incubating 200 fmol of negatively supercoiled plasmid pUC18 and 300 fmol of enzymes. Reactions were stopped by addition of 2.5 % (w/v) of SDS. Following Proteinase K digestion the samples were run on a 1% agarose gel and the bands visualized by staining with ethidium bromide. C: negative control, no enzyme added; R: relaxed DNA; SC: supercoiled DNA. (b) Purified hTop1 and heat treated hTop1 (HIPO) were analyzed by SDS-PAGE and visualized by Comassie staining. M: protein marker.

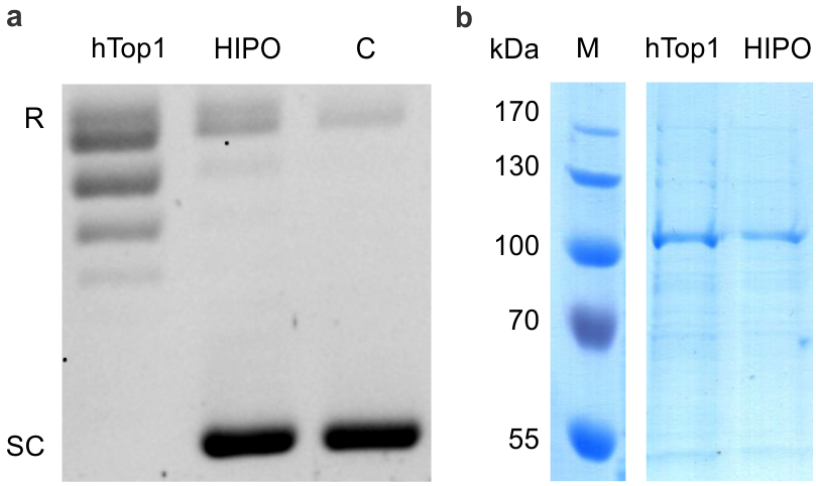


**hTop1 response in reference sensor device (without capture DNA probe)**

**Figure S3. Control experiment without capture DNA probe**. Real-time sensor response (pH7.5) of a graphene device without capture DNA probe (Gr/pABAc) to 1 nM of hTop1 (compare fig. 3(b,c)). (a) 2D map plotting $R_{gr}(V_{ecG}, t)$ (b) Real-time profile of the Dirac point extracted from (a). Upon addition of hTop1 (+ hTop1), the Dirac point appears to shift down, however it comes back to the initial value when coming back to reaction buffer (RB).

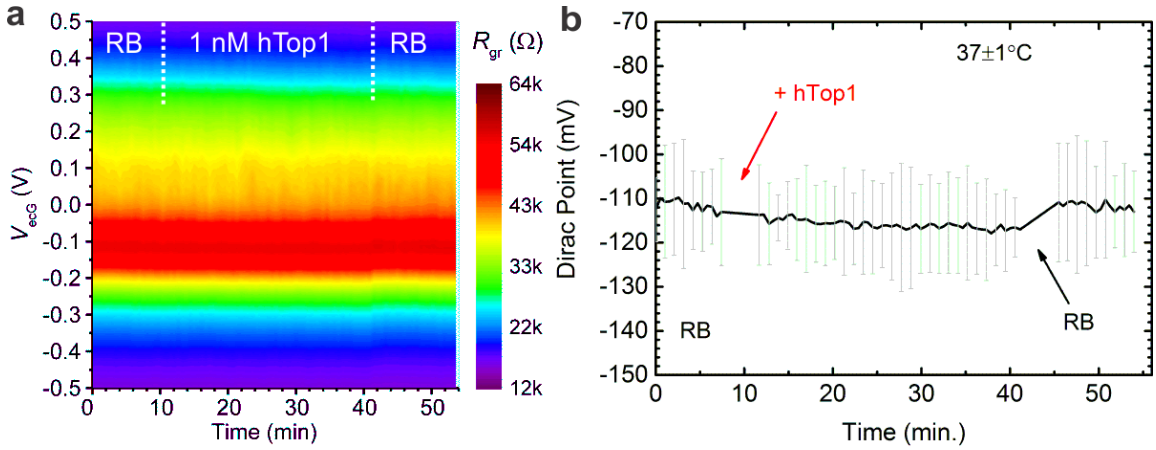


This behavior is analogous to what happens with HIPO in fig. 4, which leads us to conclude that there is only some non-specific interaction with the sensor surface in the absence of the

capture DNA probe. This interaction is mostly electrostatic since the surface in negatively charged (COOH groups of pABAc), while hTop1 is positively charged. In contrast to this, a specific interaction of hTop1 with a DNA-functionalized graphene surface leads to a persistent negative shift in Dirac point even after coming back to RB:

**Binding model for the kinetics of hTop1 interaction on immobilized DNA probe**

The kinetics of the complete catalytic cycle of hTop1 is quite complex. [5] Here, due to the clear decoupling of the two catalytic steps, we use a simple first order model similar to the ones used earlier for human topoisomerase II. [6] We assume two distinct steps for the enzyme-DNA interaction during the cleavage step, a first non-covalent interaction involving association and dissociation phases and a second covalent step, which we assume is irreversible within the time scale of our measurements. Support for the latter is gathered from the fact that we do not see a recovery of the original sensor response in the absence of hTop1. Based on these assumptions, the rate equations are modelled as done earlier [7] using an association rate constant $k_a$ and a dissociation rate constant $k_d$, with the former including the contribution for both covalent and non-covalent association of the enzyme and DNA, while the latter accounts for dissociation of the enzyme during the non-covalent interaction phase. From these parameters, the surface binding constant is computed as $K_D = k_d / k_a$. The rate equations are symbolically modelled in Mathematica and a fit of the data to the model is achieved using a non-linear fit exploiting a global optimization strategy using gradient search.

**Figure S4. Steady state response of concentration dependence**. The gate dependence of graphene resistance ($R_{gr}(V_{ecG})$) extracted from the data in fig. 6(a) is plotted at different time instances: initial in reaction buffer (black curve, RB, $t$ = 10min.), after interaction with 300 pM hTop1 (red curve, 300 pM hTop1, $t$ = 50 min.) and after interaction with 3 nM hTop1 (blue curve, 3 nM hTop1, $t$ = 85 min.)

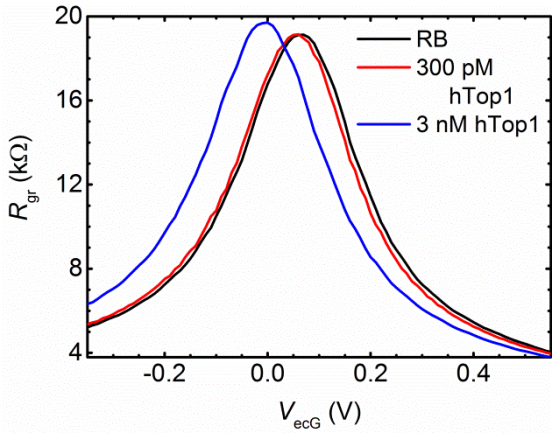


**Figure S5. Line Profiles across the AFM images** of fig. 7 at the initial stage (black line, bare graphene) and after the sensor trials (red curve, Gr/pABAc/DNA-hTop1). The line profile was taken across the graphene sheet at an area close to the lower electrode. It is apparent that after the sensor trials, many 'bumps' are discernible on the surface (in addition to the 2 to 3 nm increase in thickness that we typically see for the polymer coating) indicative of a rough surface, which we attribute to enzyme molecules left over on the graphene surface.

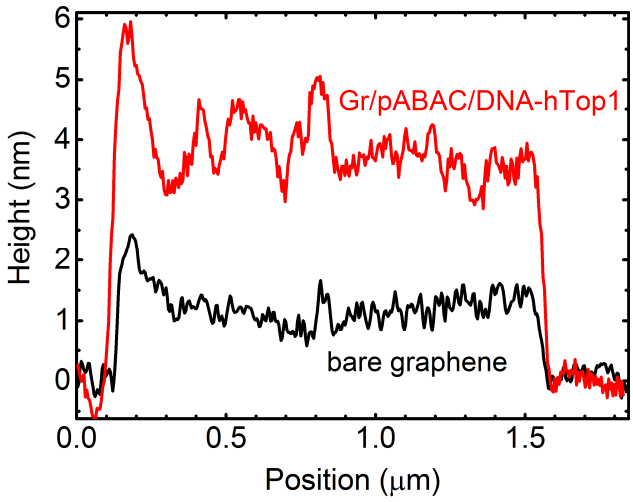

**Figure S6. Specificity of the sensor to hTop1**. Real-time sensor response of a capture-DNA (*Topo Grissino*)-functionalized graphene device to 1 nM of glucose oxidase (GOD) (a,b) and subsequently to 1 nM of hTop1 (c,d). (a) 2D maps showing $R_{gr}(V_{ecG}, t)$ and (b) real-time profile of Dirac point extracted from (a). BUF : pH 7.3 phosphate buffer. (c) 2D maps showing $R_{gr}(V_{ecG}, t)$ and (d) real-time profile of Dirac point extracted from (c) for the same device as in (a,b). RB: reaction buffer. In (a,b) there is negligible shift in Dirac point due to addition of glucose oxidase (pI : 4.2), while upon addition of hTop1, a clear and persistent shift in Dirac point consistent with other results is clearly observed.

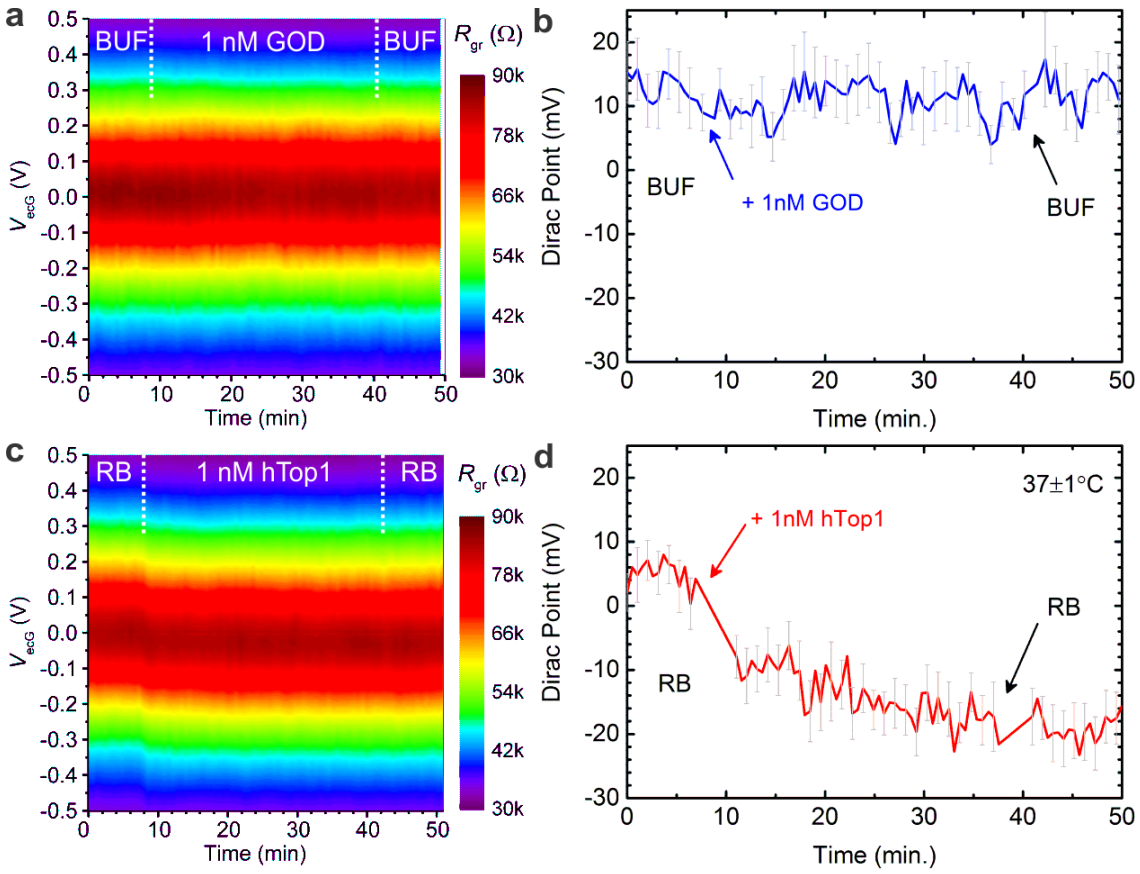


SUPPORTING REFERENCES


1. Zuccaro, L.; Kern, K.; Balasubramanian, K., Identifying Chemical Functionalization on Individual Carbon Nanotubes and Graphene by Local Vibrational Fingerprinting. *ACS Nano* **2015**, *9*, 3314-3323.

2. Zuccaro, L.; Krieg, J.; Desideri, A.; Kern, K.; Balasubramanian, K., Tuning the Isoelectric Point of Graphene by Electrochemical Functionalization. *Scientific Reports* **2015**, *5*, 11794.

3. Kurkina, T.; Vlandas, A.; Ahmad, A.; Kern, K.; Balasubramanian, K., Label-Free Detection of Few Copies of DNA with Carbon Nanotube Impedance Biosensors. *Angew. Chem. Int. Ed.* **2011**, *50*, 3710-3714.
4. Christiansen, K.; Svejstrup, A. B. D.; Andersen, A. H.; Westergaard, O., Eukaryotic Topoisomerase I-Mediated Cleavage Requires Bipartite DNA Interaction - Cleavage of DNA Substrates Containing Strand Interruptions Implicates a Role for Topoisomerase-I in Illegitimate Recombination. *J. Biol. Chem.* **1993**, *268*, 9690-9701.
5. Kristoffersen, E. L.; Jorgensen, L. A.; Franch, O.; Etzerodt, M.; Frohlich, R.; Bjergbaek, L.; Stougaard, M.; Ho, Y. P.; Knudsen, B. R., Real-Time Investigation of Human Topoisomerase I Reaction Kinetics Using an Optical Sensor: A Fast Method for Drug Screening and Determination of Active Enzyme Concentrations. *Nanoscale* **2015**, *7*, 9825-9834.
6. Renodon-Corniere, A.; Jensen, L. H.; Nitiss, J. L.; Jensen, P. B.; Sehested, M., Interaction of Human DNA Topoisomerase Ii Alpha with DNA: Quantification by Surface Plasmon Resonance. *Biochemistry* **2002**, *41*, 13395-13402.
7. Oshannessy, D. J.; Brighamburke, M.; Soneson, K. K.; Hensley, P.; Brooks, I., Determination of Rate and Equilibrium Binding Constants for Macromolecular Interactions Using Surface-Plasmon Resonance - Use of Nonlinear Least-Squares Analysis-Methods. *Anal. Biochem.* **1993**, *212*, 457-468.